CERN EUROPEAN ORGANIZATION FOR NUCLEAR RESEARCH

CERN/ISRC 75-43
3 November, 1975

M E M O R A N D U M

To: I.S.R.C.

From: R605 Collaboration

Subject: Capabilities of the proposed set-up for electron identification

---

According to the minutes of the 60th meeting of the ISRC:

"The group is requested to provide the Committee with a more detailed description of the capabilities of the proposed set-up for electron identification and to clarify with the CERN administration several points concerning available resources for support".

The present document deals with the question of the electron identification.

As pointed out in proposal (ISRC/75-33) the various elements of the new detector have expected performances which are very close or better than the ones of the corresponding elements of the present set-up. Electrons will then be identified unambigously from other charged tracks at the expected level of 10^{-4}.

Additional detectors in both set-ups separate electrons directly produced from many recognized secondary sources like Dalitz pairs, pairs produced in the vacuum chamber, compton electrons and decay electrons from known β-decays. We believe that results are expected to be closely identical since the future vacuum chamber will be even more adapted to the experiment and the geometry of the new auxiliary counters is such that cuts can be kept virtually the same as the ones presently in use.

The only way in which we can interpret the concern of the members of the ISRC is because whilst the old telescope covered angles from 25^{o} to 40^{o} (fig. 1), the new detector now extends down to 11^{o}. Note that 11^{o} represents

CR/ef

a limiting ray and probably a more realistic detection angle is in the vicinity of 14^{o} (fig. 2). Then, the question of the ISRC can be explicited as follows:

"Can the selection criteria which have been proven to work from 40^{o} to 25^{o} be applicable down to 14^{o} (11^{o})? ($0.2 < p_t < 1$ GeV/c)".

1. GENERAL DISCUSSION ON SELECTION CRITERIA FOR THE NEW SET-UP

There are several possible sources of spurious electrons (positrons):

(a) Dalitz pairs with one of the particles of the pair unidentified.

(b) Real pairs due to conversion in the vacuum chamber walls and subsequent loss (multiple scattering) of one of the members of the pair.

(c) Compton electrons (only negative).

(d) Electrons (positrons) from semi-leptonic decays of known particles (like $K^{\pm}$, K^{o}, Λ^{o} and so on).

Background (c) cannot be further reduced. Background (a), (b) and (d) are minimized in the present set-up by requiring no other charged track over a "guard" solid angle. This is realized by a pulse height requirement in the trigger counter hit by the identified electron and by an anticoincidence requirement in the neighboring counters. It is foreseen to use the same "guard" solid angle around the electron (positron) in the new set-up. In fact, this is made easier by the larger area drift chambers. Therefore, backgrounds remain the same for the same vacuum chamber thickness and for overlapping angular range $25^{o} < \theta < 40^{o}$. In practice, the vacuum chamber is on average $\sim$ 50% thinner for the new arrangement and this can only lead to improvements. We have estimated in detail the dependence of the background (a) - (d) on θ and found a relatively smooth dependence which guarantees that the same favourable background conditions persist down to 11^{o} and for the whole specified transverse momentum range $0.2 < p_t < 1.0$ GeV/c. This is relatively trivial to understand in the case of background (a), i.e. Dalitz pairs, since smaller angles at constant p_t simply reduces the opening angle of pairs like 1/p and hence it only increases the efficiency of the "guard" solid angle.

More sophisticaled are the effects on backgrounds (b) to (d) and they must be discussed in greater detail. This is the topic of the next sections.

2. PRODUCTION AND MULTIPLE SCATTERING OF e^+e^- PAIRS

This background process consists of the production of a photon from $\pi^o \to \gamma + \gamma$ decay followed by conversion of the photon in the vacuum chamber with one of the members of the pair lost. The event simulates the production of a direct $e^{\pm}$. We shall discuss the relevant cross sections in order to derive a scaling law which will give the background dependence on the angles of the telescope.

2.1 The Bethe-Heitler formula

The classic formula is expressed by several joining equations, linked through the screening parameter γ:

$$\gamma = 100 \frac{m_e}{E_\gamma (1-u)u} \frac{1}{Z^{1/3}}$$

where
- Z = atomic number (26 for steel)
- m_e = electron mass
- E_γ = gamma energy
- u = E_e/E_γ

For our problem there are four regions of interest. The absolute probability for radiation length and per unit du is given by:

$$\frac{dP}{du} (E_\gamma, E_-), \text{ where}$$

(a) $$\frac{dP}{du} = \frac{1}{\ln\left(\frac{183}{Z^{1/3}}\right)} \left\{u^2 + (1-u)^2 + \frac{2}{3}u(1-u)\right\}\left\{\ln\frac{2E_\gamma}{m_e}(u(1-u)) - \frac{1}{2}\right\}$$

for

$\gamma \geq 15$

(b) $$\frac{dP}{du} = \frac{1}{\ln\left(\frac{183}{Z^{1/3}}\right)} \left\{u^2 + (1-u)^2 + \frac{2}{3}u(1-u)\right\}\left\{\ln\frac{2E_\gamma}{m_e}\, u(1-u) - c(\gamma)\right\},$$

$15 > \gamma \geq 2$

where

$$c(\gamma) \simeq 0.21\left\{\left(\frac{\gamma}{2}\right)^{-1.23} - \frac{1}{200}\left(\frac{\gamma}{2} - 1\right)^{1.20}\right\}$$

(c)

$$\frac{dP}{du} = \frac{1}{\ln\left(\frac{183}{Z^{1/3}}\right)} \left\{u^2 + (1-u)^2 + \frac{2}{3}u(1-u)\right\}\left\{\frac{19.6 - 1.9\gamma}{4} - \frac{1}{3}\ln Z\right\},$$

$2 > \gamma \geq .8$

(d)

$$\frac{dP}{du} = \frac{1}{\ln\left(\frac{183}{Z^{1/3}}\right)} \left[\left\{u^2 + (1-u)^2\right\}\left\{\frac{20.8 - 3.5\gamma}{4} - \frac{1}{3}\ln Z\right\} + \right.$$
$$\left. + \frac{2}{3}(u(1-u))\left\{\frac{20.3 - 2.875\gamma}{4} - \frac{1}{3}\ln Z\right\}\right],$$

$.8 > \gamma \geq .01$

The above is to be contrasted with the standard simple approximate formulae:

$$\frac{dP}{du} = \frac{7}{9}\ .$$

Since most of our multiple scattering contributions will be shown to come from momentum less than $\sim$ 20 MeV/c, it turns out to be numerically important to use the more complicated Bethe-Heitler formalism. This is demonstrated in fig. 3, where we consider the probability distribution:

$$\frac{dP}{dp_e} = \frac{p_e}{E_e} \frac{dP}{du} \cdot \frac{1}{E_\gamma}$$

for steel. It is more instructive to plot it in terms of

$$E_\gamma \frac{dP}{dp_e} = \frac{p_e}{E_e} \frac{dP}{du} ,$$

since it is the momentum of the electron which plays the key role in the multiple scattering. We plot the curves for $p_e < 70$ MeV/c and $E_\gamma = 400$, 800 and 2000 MeV.

We note that for low p_e, the product $E_\gamma \, dP/dp_e = d\pi/dp_e$ is independent of E_γ, and that the mean value of the probability x E_γ is considerably less than the simplified value 7/9. Thus, it is critical in any estimate to use the correct pair formula, translated in the suitable language for our problem, i.e. $d\pi/dp_e$ rather than dP/du.

2.2 Multiple scattering

The multiple scattering can deviate one of the members of the pair sufficiently to miss the telescope. Hence, the event will look identical to the direct emission of an electron (positron). In order to simplify the symbolism we shall assume that e^+ are to be detected and hence that the background event is due to the loss of the e^-. In order to derive the scaling law we shall assume furthermore that the probability of loosing the e^- is independent of the angle of the telescope, i.e.: $\beta(p_-)$. The function $\beta(p_-)$ is a complicated but a priori known function of p_-; it is furthermore independent of p_+, since the opening angle of the pair due to Bethe-Heitler is negligible with respect to multiple scattering.

2.3 Production formulae

For the range of values of interest to us, we can safely state:

$$\boxed{\left.\frac{dN}{dE}\right|_{\pi^+} = \left.\frac{dN}{dE}\right|_{\pi^0} = b^2 E e^{-bE}}$$

where b = 6 sinθ, E in GeV, i.e. we assume an equal number of π^+ and π^o at the production angle θ and cnergy E.

We shall assume also that γ-rays from π^o follow the π^o direction. Note that this assumption improves as we go to higher energy π^o's. The conclusion from the above statements is that:

$$\frac{dN}{dE_\gamma} = 2 \times \int_{E_{\pi^o}=E_\gamma}^{\infty} (dN)_{\pi^o} \times \frac{1}{E_{\pi^o}} = 2 \times \int_{E_{\pi^o}=E_\gamma}^{\infty} b^2 e^{-bE_{\pi^o}} E_{\pi^o}/E_{\pi^o} \times dE_{\pi^o}$$

$$= 2be^{-bE_\gamma}$$

Thus:

$$\boxed{\frac{dN}{dE_\gamma} = 2be^{-bE_\gamma}}$$

Note the factor of 2 which comes from $\pi^o \rightarrow 2\gamma$.

2.4 Estimate of the background rate

The yield of background positrons, dN/dE_+ is obtained as an integral over the γ-ray spectrum:

$$\frac{dN}{dE_+} \simeq \int_{E_\gamma = m_e + E_+}^{\infty} \frac{dN}{dE_\gamma} dE_\gamma \qquad \frac{dP}{dp_-} \beta(p_-)$$

where $p_- \cong E_- = E_\gamma - E_+$. Replacing variables and within the relativistic approximations:

$$\frac{dN}{dE_+} \simeq \int_{m_e}^{\infty} 2be^{-b(E_+ + p_-)} \frac{dP}{dp_-} \beta(p_-) dp_-$$

$$= be^{-bE_+} \times 2 \int_{m_c}^{\infty} \frac{dP}{dp_-} \beta(p_-) dp_-$$

Thus:

$$\frac{dN}{dE_+} = b\, e^{-bE_+} \frac{\Gamma}{E_+}$$

where $\Gamma = 2 \int_{m_e}^{\infty} \frac{d\pi}{dp_-} \beta(p_-)\, dp_-$

is a numerical constant independent of E_+ and of the angle of the telescope. The exact value of Γ is obtained by Monte Carlo calculations based on the geometry of the detector and the B.H. formula.

The final background rate will then be:

$$\frac{dN}{dE_+}(E_+ = E) \Big/ \frac{dN}{dE_{\pi^+}}(E_{\pi^+} = E) = \frac{b\, e^{-bE} \frac{\Gamma}{E}}{b^2 e^{-bE} E}$$

$$= \frac{\Gamma}{bE^2}$$

Thus

$$\boxed{\frac{dN}{dE_{e^+}} \Big/ \frac{dN}{dE_{\pi^+}} = \frac{\Gamma \sin\theta}{6\, p_t^2}}$$

where $p_t \simeq E \sin\theta$ is the transverse momentum. To conclude: <u>The contribution of background due to real pairs is directly proportional to sinθ and inversely proportional to the square of the transverse momentum.</u>

3. APPARENT ELECTRON (e^-) SIGNAL DUE TO COMPTON EFFECT

This background is produced by Compton electrons in the vacuum chamber walls and other material of the detecting apparatus. Since the photon is generally missed, the effect simulates the "direct" production of e^-. In order to shorten the discussion a simple scaling law is derived, folding the $\pi^0 \to 2\gamma$ spectrum with the Compton formula.

3.1 Compton formula

Let us define some variables:

$E \equiv$ initial photon energy

$E' \equiv$ final photon energy

$E_e = E - E' \equiv$ total electron energy

$\phi \equiv$ final photon direction

Then we can show from energy and momentum conservation that

$$E' = \frac{m_e E}{m_e + E\,(1 - \cos\phi)}$$

Then: $m_e/2 < E' \leqslant E$, where we have neglected terms of order $(m_e/E)^2$.

Let us traverse a thickness of steel of 1 g/cm^2 and define the constant $C = \pi N(Z/A)\, r_o^2 = 0.150\,(Z/A)$ (N = Avogadro's number, r_o = classical electron radius, Z, A = atomic constants of the material). The differential probability to produce a Compton electron is given by:

$$\frac{dP}{dE'}(E, E') = C\,\frac{m_e}{E}\,\frac{1}{E'}\left[1 + \left(\frac{E'}{E}\right)^2 - \left(\frac{E'}{E}\right)\sin^2\phi\right]$$

$$= C\,\frac{m_e}{E}\left[\frac{1}{E'}\left(1 - \frac{m_e}{E}\left(1 - \frac{E'}{E}\right)\right)^2 + \frac{E'}{E^2}\right]$$

Ignoring terms in $m_e/E \leqslant 0.5/400 \simeq 10^{-3}$ with negligible effects, we now re-write the formula in terms of the electron energy $E_e = E-E'$:

$$\frac{dP_e}{dE_e}(E_e, E) = C\frac{m_e}{E}\left\{\frac{1}{E-E_e} + \frac{E-E_e}{E^2}\right\}$$

We wish to fold the γ-ray spectrum of sect. 2.3 with the above formula and integrate over E_γ from $E_e + m_e/2$ to ∞:

$$\frac{dN}{dE_e} = 2C\, m_e \int_{E_\gamma = E_e + m_e/2}^{\infty} \frac{1}{E_\gamma^2}\left[\frac{1}{1-E_e/E_\gamma} + 1 - \frac{E_e}{E_\gamma}\right] b\, e^{-bE_\gamma}\, dE_\gamma$$

Defining $x_o = b\,E_e$ and $\delta = b\,m_e/2$ we can transform the formula into the following expression:

$$\frac{dN}{dE_e} = 2C\, m_e \int_{x_o+\delta}^{\infty} \frac{e^{-x}}{x}\left(\frac{1}{x-x_o} + \frac{x-x_o}{x^2}\right) dx$$

Now we introduce the variable $y = x-x_o$ and obtain:

$$\frac{dN}{dE_e} = 2C\, m_e b^2 \frac{e^{-x_o}}{x_o} \int_{\delta}^{\infty} \frac{e^{-y}}{y}\left(\frac{x_o}{x_o+y}\right)\left(\frac{1+y^2}{(x_o+y)^2}\right) dy$$

$$= 2C\, m_e b^2 \frac{e^{-x_o}}{x_o}\left[I_1(x_o) + I_2(x_o)\right]$$

where:

$$I_1(x_o) = \int_{\delta}^{\infty} \frac{e^{-y}}{y}\,\frac{x_o}{x_o+y}\, dy$$

$$I_2(x_o) = \int_{\delta}^{\infty} \frac{e^{-y}}{y}\,\frac{x_o y^2}{(x_o+y)^3}\, dy$$

The evaluation of these integrals is very laborious and is not reported here. The members of the ISRC Committee are invited to contact directly the group for complete details. The result is expressed in terms of the basic integral:

$$ei(x) = \int_x^\infty \frac{e^{-y}}{y}\,dy = -\left\{\gamma + \ln x + \sum_{n=1}^{\infty} \frac{(-x)^n}{n\,n!}\right\}$$

where γ = Euler's constant, 0.577215. Clearly for $x << 1$, $ei(x) \rightarrow -(\gamma + \ln x)$.

$$I_1(x_0) = ei(\delta) - e^{x_0}\, ei(x_0 + \delta)$$

$$I_2(x_0) = (1 + x_0)/2 - x_0 e^{x_0} \left(1 + \frac{x_0}{2}\right) ei(x_0)$$

Putting it all together we get:

$$\boxed{\frac{dN}{dE_e} = 2C \frac{m_e}{E_e} e^{-bE_e} \left\{ ei\left(\frac{b m_e}{2}\right) + \frac{1 + bE_e}{2} - ei(bE_e)\, e^{bE_e}\left[1 + bE_e + \frac{(bE_e)^2}{2}\right]\right\}}$$

Replacing $ei(x) \simeq -(\gamma + \ln x)$ and using a polynomial expression for the (bE_e) terms, valid to better than 1% over the interval of interest to us gives the final formula:

$$\frac{dN}{dE_e} = \frac{2C(m_e b)\, b\, e^{-bE_e}}{bE_e} \left\{ .577 - \ln\left(\frac{b m_e}{2}\right) - .75\left[\frac{1}{bE_e} + \frac{bE_e}{(1 + bE_e)^3}\right]\right\}$$

If we divide the above formula by the π^- spectrum of sect. 2.3 and use the definition of b in terms of the production angle θ we get:

$$\frac{dN}{dE_e}(E_e = E) \Big/ \frac{dN}{dE_\pi}(E_\pi = E) = .99 \times 10^{-3}\, b\left(\frac{t}{t_R}\right) \Big/ (bE)^2$$

$$\times \left\{ 6.59 + \ln \sin\theta - 0.75\left[\frac{1}{bE_e} + \frac{bE_e}{(1+bE_e)^2}\right]\right\}$$

where we have expressed the steel thickness in terms of the radiation length (t_R = 17.6 mm). Note that the term within { } is practically constant and in a very good approximation:

$$\left(\frac{e}{\pi}\right)_{COMPTON} \propto \frac{1}{bE^2} \quad \text{or} \quad \propto \frac{\sin\theta}{b\, p_t^2}$$

where $p_t = E \sin\theta$ is the observed transverse momentum.

4. PRODUCTION AND WARK SEMI-LEPTONIC DECAY OF "ORDINARY" PARTICLES

Electrons could be simulated by the leptonic decay of $K^\pm$, K^o and so on. We shall initially assume that the decay path before the detector is short with respect to the natural decay path. Normally, they undergo multibody decays of the form:

$$A \rightarrow B + e + \nu \; .$$

We shall assume that A is not polarized. Hence the decay distribution of the electrons is fully determined by the decay spectrum in A center of mass, dN/dp_e^*. The detailed knowledge of this spectrum is not necessary in the formulation of scaling laws at different telescope angles. We shall however make the relativistic approximation for the electron in the center of mass i.e. $E_e^* \simeq p_e^*$.

Let us first consider the relative probabilities in the laboratory system for one electron of momentum p_e^* in the center of mass. The Lorentz transformation is, as usual:

$$E_e = \gamma\,(\beta p_e^* \cos\Theta^* + E_e^*) \simeq \gamma p_e^* (\beta\cos\Theta^* + 1)$$

where β and γ refer to particle A. Since e is distributed isotropically in the A rest frame we can write:

$$\frac{dP}{dE_e} = \frac{1}{E_{MAX} - E_{MIN}} = \frac{M_A}{2E_A p_e^* \beta} = \frac{M_A}{2 p_A p_e^*}$$

where:

$$E_{MAX} = \gamma p_e^* (\beta + 1) = \frac{E_A}{M_A} p_e^* (1+\beta)$$

and

$$E_{MIN} = \frac{E_A}{M_A} p_e^* (1-\beta)$$

With the reasonable assumption that $1 + \beta \simeq 2$ the expressions for E_{MIN}, E_{MAX} can be further simplified:

$$\boxed{E_{MAX} \simeq \frac{2E_A}{M_A} p_e^*}$$

$$E_{MIN} \simeq \frac{E_A}{M_A}\frac{p_e^*}{2}(1-\beta)(1+\beta) = \frac{E_A}{2M_A} p_e^* (1-\beta^2)$$

$$= \frac{E_A}{2M_A} p_e^* \frac{1}{\gamma^2}$$

Thus:

$$\boxed{E_{MIN} = p_e^* \frac{M_A}{2E_A}}$$

The actual number of electrons per unit of electron energy is easily calculated as an integral over p_e^* and taking into account the decay probability $B\,\ell^*/c\tau$, where B is the decay branching ratio, ℓ^* is the potential decay length in the centre of mass and $c\tau$ is the lifetime factor:

$$\frac{dN_e}{dE_e} = \int_0^{M_A/2} dp_e^* \int_{E_A(MIN)}^{E_A(MAX)} dE_A \frac{dN_A}{dE_A} \cdot \frac{dP}{dE_e} \cdot \frac{dN}{dp_e^*} \cdot \frac{B \cdot \ell \cdot M_A}{c\tau\, p_A}$$

where $E_A(MAX) = \frac{E_e M_A}{p_e^* (1-\beta)}$ and $E_A(MIN) = \frac{E_e M_A}{p_e^* (1+\beta)}$

Putting all terms orderly together we get:

$$\frac{dN}{dE_e} = \int_0^{M_A/2} dp_e^* \int_{\frac{E_e M_A}{2 p_e^*}}^{\frac{E_e M_A}{p_e^*(1-\beta)}} dE_A \; b^2 \, e^{-bE_A} \, E_A \frac{M_A}{2 p_A p_e^*} \frac{dN}{dp_e^*}(p_e^*) \frac{B \ell M_A}{p_A c \tau}$$

Making a relativistic approximation for particle A we get:

$$\frac{dN}{dE_e} = \int_0^{M_A/2} dp_e^* \int_{E_e \frac{M_A}{2 p_e^*}}^{\infty} dE_A \, b^2 \, e^{-bE_A} \frac{1}{2E_A} \cdot \frac{M_A^2 B \ell}{c \tau p_e^*} \frac{dN}{dp_e^*}(p_e^*)$$

$$\boxed{\frac{dN}{dE_e} = \frac{M_A^2 B \ell}{2 c \tau} \int_0^{M_A/2} \frac{dp_e^*}{p_e^*} \frac{dN}{dp_e^*}(p_e^*) \int_{E_e \frac{M_A}{2 p_e^*}}^{\infty} dE_A \, b^2 \frac{1}{E_A} e^{-bE_A}}$$

Introducing a simple variable substitution in the second part of the integral, $y = -bE_A$, leads to the following expression:

$$\frac{dN}{dE_e} = \frac{M_A^2 B \ell}{2 c \tau} b^2 \int_0^{M_A/2} \frac{dp_e^*}{p_e^*} \frac{dN}{dp_e^*}(p_e^*) \int_{y_0}^{\infty} dy \frac{e^{-y}}{y}$$

with

$$y_0 = \frac{b E_e M_A}{2 p_e^*} = \frac{8 \sin\theta \, E_e M_A}{2 p_e^*} \approx 4 p_\perp \frac{M_A}{p_e^*}$$

The integral in y has already been discussed in sect. 3.1:

$$ei(y_0) = \int_{y_0}^{\infty} dy \frac{e^{-y}}{y} = -\left\{ \gamma + \ln y_0 + \sum_{N=1}^{\infty} \frac{(-y_0)^N}{N N!} \right\}$$

with γ = 0.577215, the Euler's constant.

Finally, the electron spectrum has the form:

$$\frac{dN}{dE_e} = \frac{M_A^2 B \ell}{2 c \tau} b^2 \int_0^{M_A/2} \frac{dp_e^*}{p_e^*} \frac{dN}{dp_e^*}(p_e^*) \, ei\left(4 p_\perp \frac{M_A}{p_e^*}\right)$$

Thus:

$$\boxed{\frac{dN}{dE_e} = \frac{M_A^2 B \ell}{2 c \tau} b^2 \, \Phi\left(p_\perp, \text{decay spectrum of } A\right)}$$

where we have defined:

$$\Phi = \int_0^{M_A/2} \frac{dp_e^*}{p_e^*} \frac{dN}{dp_e^*}(p_e^*) \, ei\left(4 p_\perp M_A / p_e^*\right)$$

We can now compare the electron and pion spectra for the same momentum:

$$\left(\frac{e}{\pi}\right) = \frac{dN}{dE_e}(E_e = E) \Big/ \frac{dN}{dE_\pi}(E_\pi = E) = \frac{M_A^2 B \ell}{2 c \tau} b \, \Phi \Big/ b^2 E \, e^{-bE}$$

$$= \frac{M_A^2 B \ell}{2 c \tau E} \Phi \Big/ e^{-6 p_\perp}$$

which provides the following scaling law, valid for constant p_t, different angles and arbitrary decay matrix elements:

$$\boxed{\frac{e}{\pi} \propto \frac{1}{E} \propto \sin \Theta \quad \text{for constant } p_\perp}$$

5. CONCLUSIONS

The dependence of the backgrounds for a constant p_t and different angles is summarized in table I. It appears that in general the background conditions are <u>improving</u> towards smaller angles.

Therefore, on the basis of the present experiment (fig. 4) we do not anticipate additional problems of electron detection for the new set-up.

TABLE I

Angular dependence of (e/π) background at constant apparent p_t and for constant "guard" solid angle and vacuum chamber thickness.

PROCESS	(e/π) - Ratio dependence on angle of production	Background at 11°/ Backbround at 30°
- Dalitz pairs	$\sim \sin^2\theta$	$\sim$ 0.145
- Real pairs in the vacuum chamber	$\sim \sin\theta$	0.38
- Compton electrons in the vacuum chamber	$\sim \sin\theta$	0.38
- semi-leptonic decay of known particles	$\sim \sin\theta$	0.38

FIGURE CAPTIONS

Fig. 1 Angular distributions of particles detected in R605-I electron telescope.

Fig. 2 General layout of R605-II showing (dotted lines) the acceptance in polar angle.

Fig. 3 Exact probability distribution of electron momentum, normalized to photon energy, according to the Bethe-Heitler formula for pair production.

Fig. 4 Dependence on transverse momentum of the various backgrounds in R605-I.

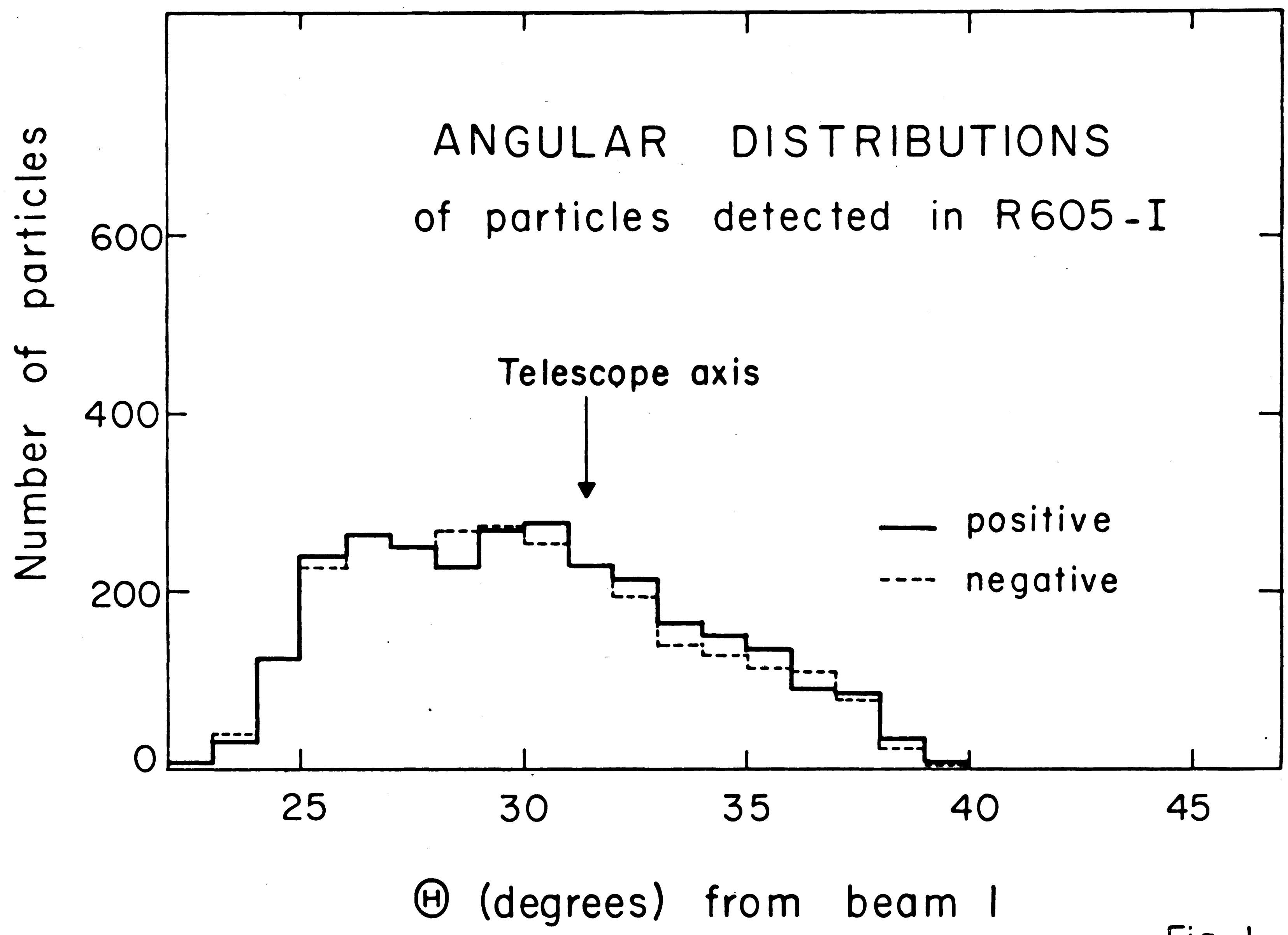
ANGULAR DISTRIBUTIONS
of particles detected in R605-I
Telescope axis
positive
negative
Number of particles
0
200
400
600
25
30
35
40
45
Θ (degrees) from beam I

Fig. 1

R 605 - II : General Layout

(vertical cut through beam / axis)

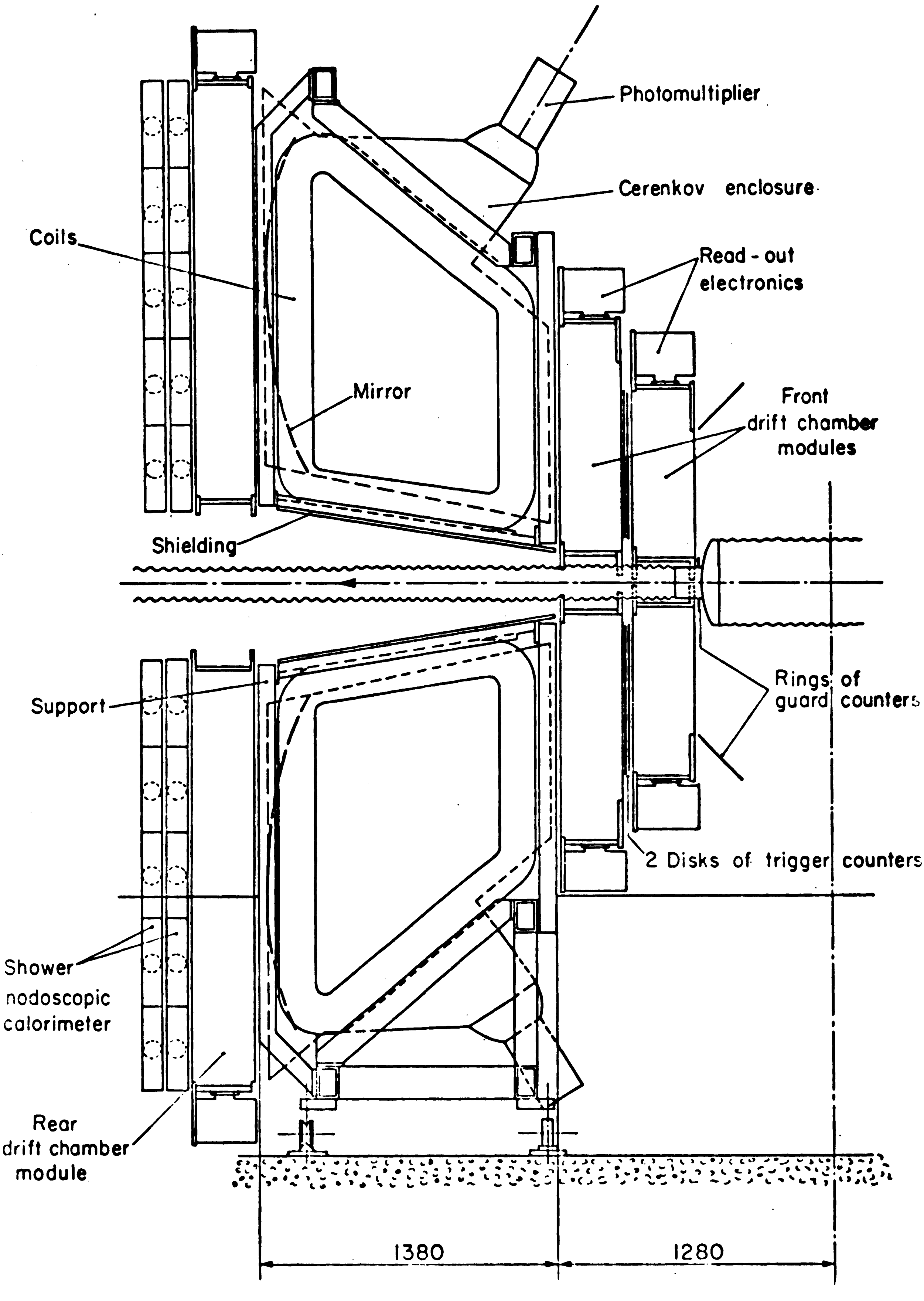

FIG. 2

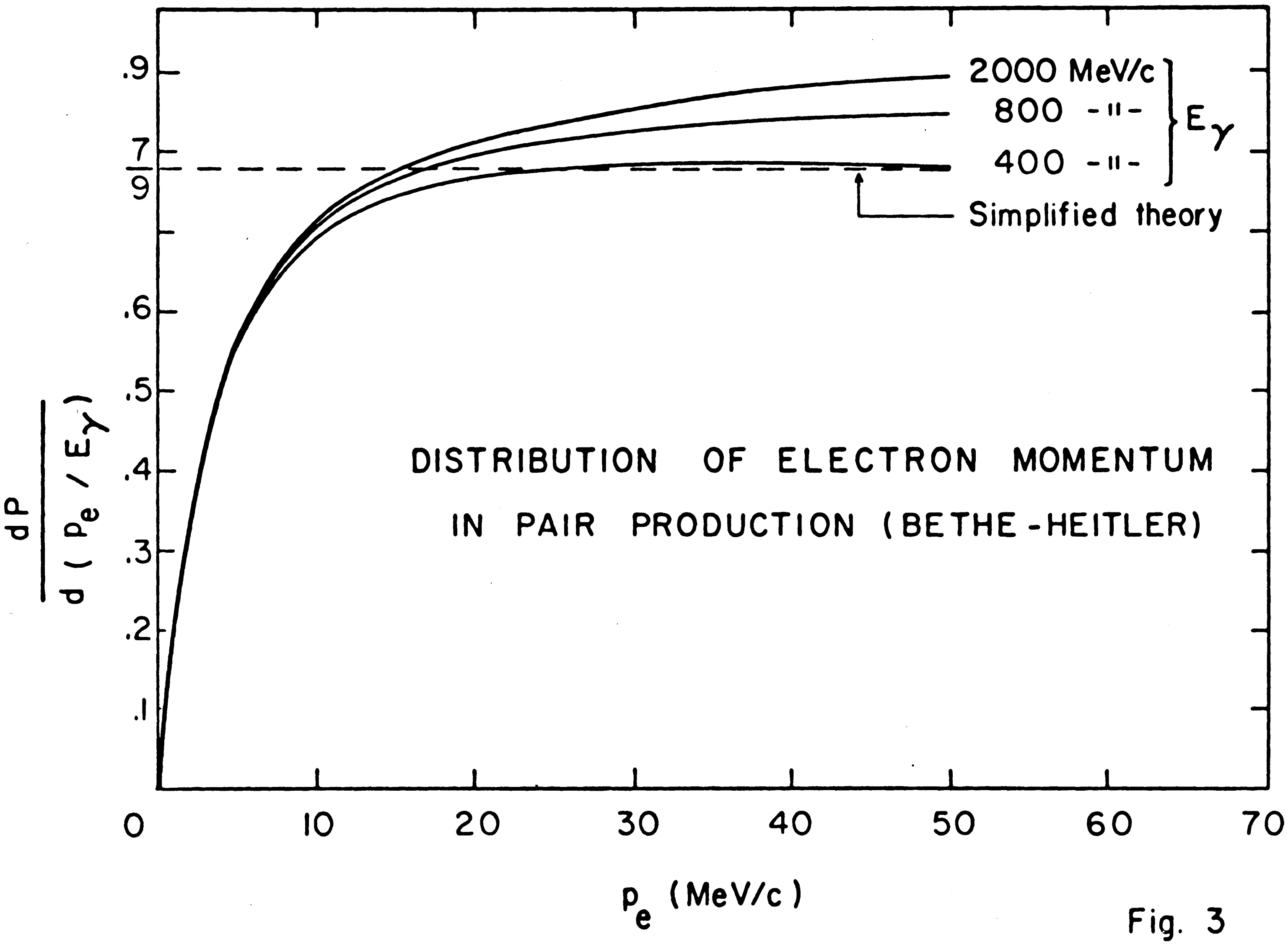
2000 MeV/c
800 -"-
400 -"-
E_γ
Simplified theory
DISTRIBUTION OF ELECTRON MOMENTUM
IN PAIR PRODUCTION (BETHE-HEITLER)
.9
7/9
.6
.5
.4
.3
.2
.1
0
10
20
30
40
50
60
70
dP / d(p_e / E_γ)
p_e (MeV/c)

Fig. 3

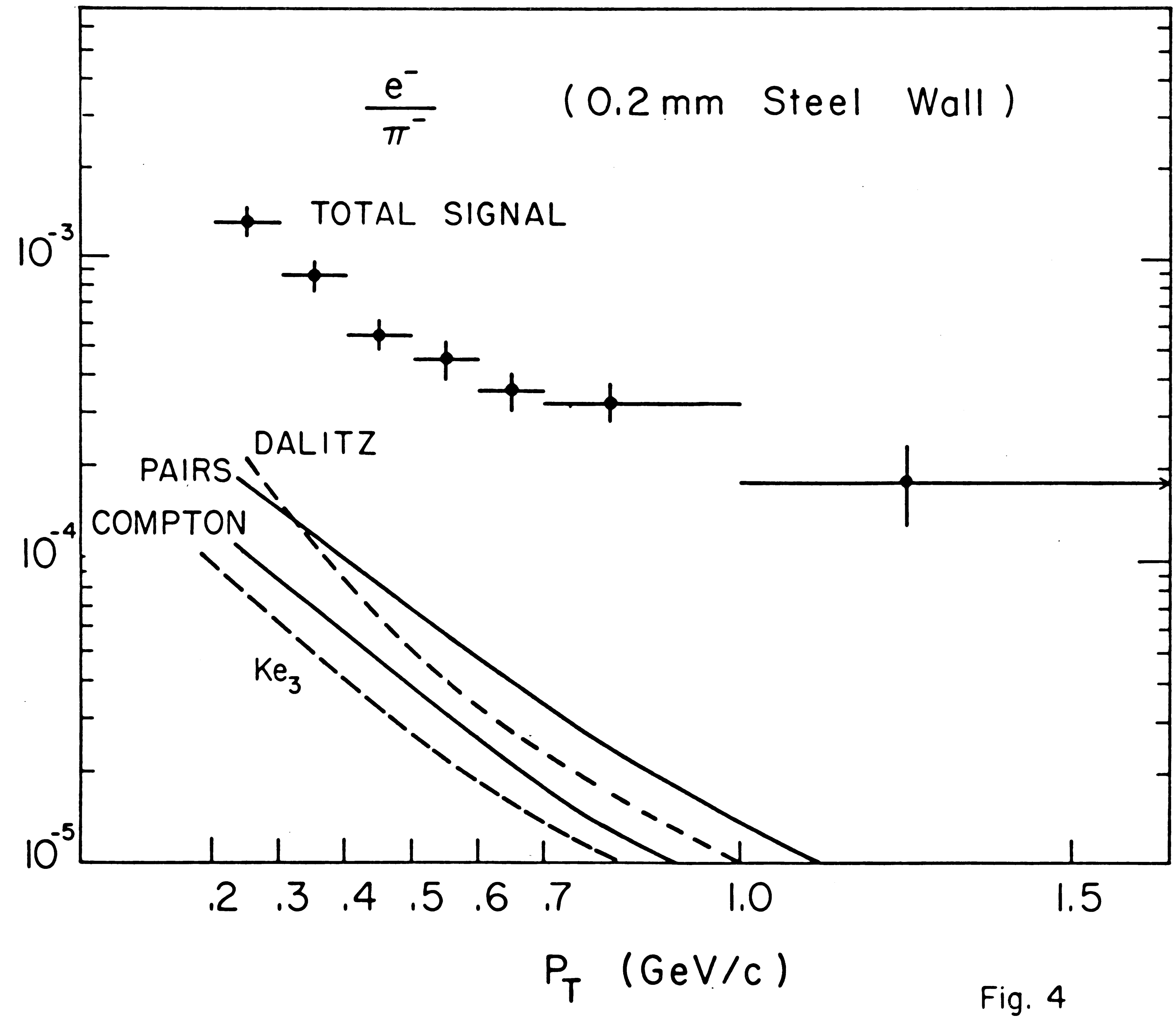

e^-/π^-
(0.2 mm Steel Wall)
TOTAL SIGNAL
DALITZ
PAIRS
COMPTON
Ke_3
10^{-3}
10^{-4}
10^{-5}
.2
.3
.4
.5
.6
.7
1.0
1.5
P_T (GeV/c)

Fig. 4

THIN VACUUM CHAMBER WALLS

R 605 - I

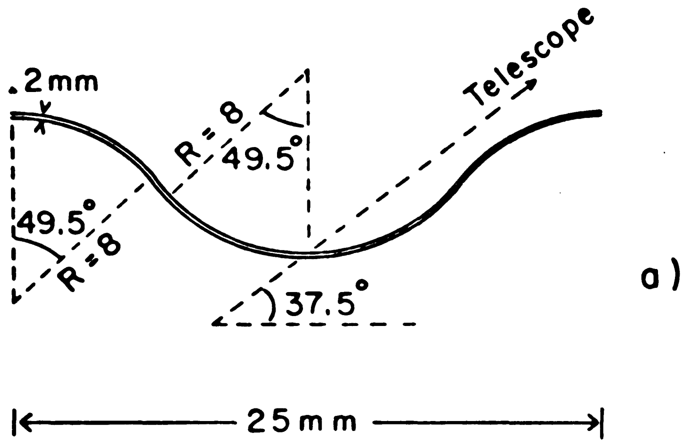

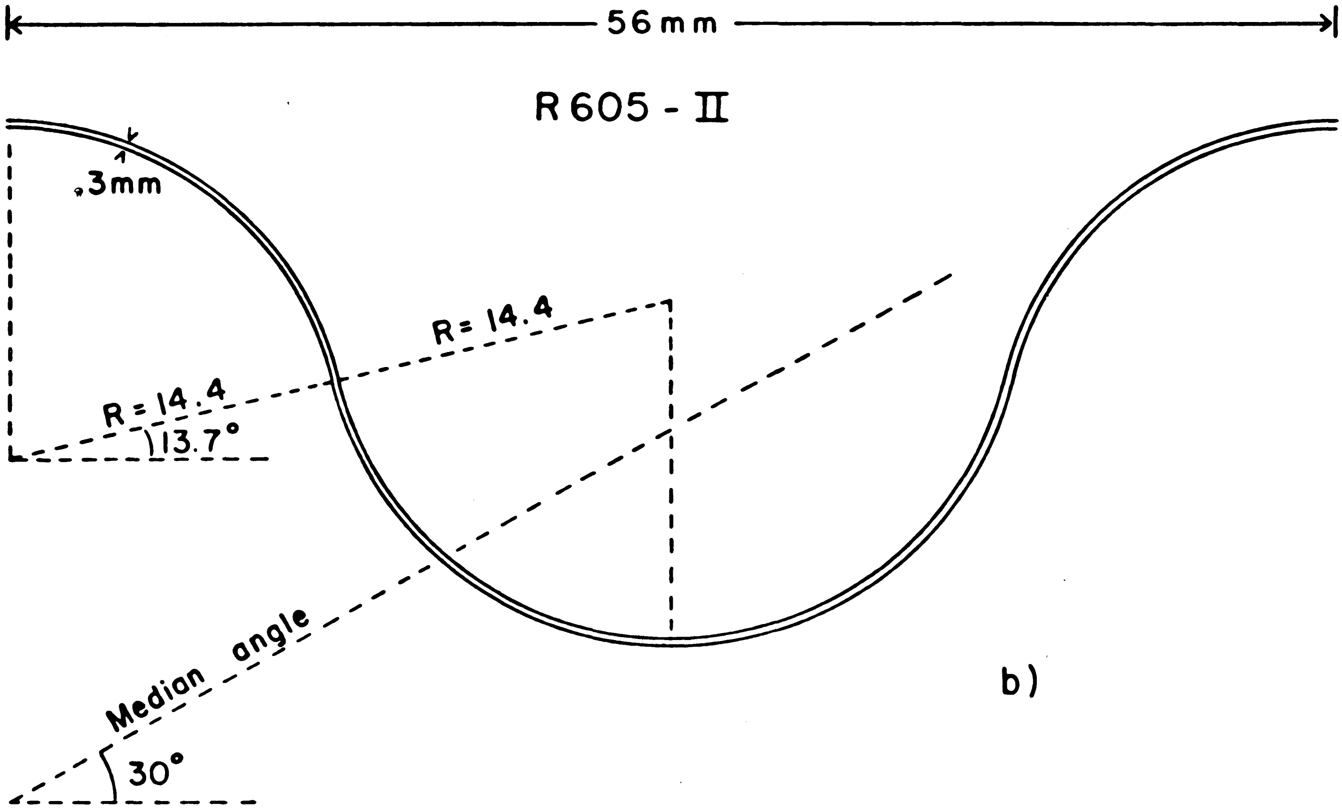

Scale 5:1

Fig. 5